

## Note

Change of handedness in cholesteric liquid crystalline phase for *N*-phthaloylchitosan solutions in organic solvents

Yanming Dong,\* Yusong Wu, Yaqing Zhao, Huiwu Wang, Yonghong Ruan, Hui Zhang, Xueming Fang

*Department of Materials Science and Engineering, State Key Laboratory for Physical Chemistry of Solid Surfaces, Xiamen University, Xiamen 361005, PR China*

Received 7 January 2003; received in revised form 29 March 2003; accepted 14 May 2003

## Abstract

The influence of concentration on the helicoidal change of *N*-phthaloylchitosan (PhCh) solutions in Me<sub>2</sub>SO, DMAc and DMF was investigated by means of circular dichroism (CD). The critical concentrations to form liquid crystal phase in these three solvents were 43, 45 and 48 wt.%, respectively as measured with polarized optical microscope. There were two kinds of CD peaks, sharp peaks with absorption maximum at about 330 nm induced by the helical conformation of molecular chain, and very broad peaks covering almost whole visible region induced by the cholesteric helix of mesophase. The later only appeared in concentrated solutions with the concentration higher than the critical concentration. The handedness of both levels of helicoidal structures changed from left- to right-handed with the increase of concentration for PhCh/Me<sub>2</sub>SO solutions. The chirality transfer occurred between these two chiral levels. For PhCh/DMAc and PhCh/DMF systems, only the handedness of helical conformation reversed, but the cholesteric helix did not change. As a method to measure critical concentration, CD is more sensitive than polarized optical microscopy (POM).

© 2003 Elsevier Ltd. All rights reserved.

**Keywords:** *N*-Phthaloylchitosan; Cholesteric liquid crystals; Circular dichroism; Handedness; Conformation

## 1. Introduction

Chitin, the principal component of the supporting structure of living organisms such as fungi, algae, annelids, molluscs and arthropods is one of the most important polysaccharides having the repeating structural unit of 2-acetamido-2-deoxy- $\beta$ -D-glucose.<sup>1</sup> This naturally occurring polymer yields chitosan when partially or fully deacetylated. Chitosan has a free amino group which promotes its solubility in acidic solvents. But chitosan does not dissolve in common organic solvent because of strong hydrogen bond interactions between chains. *N*-Phthaloylchitosan (PhCh) is one of the regioselectively chemically modified chitosan, with a high solubility in common organic solvents.<sup>2,3</sup> It is

especially suitable for the investigation of lyotropic liquid crystals.

It is well known that cellulose and some derivatives form both lyotropic and thermotropic liquid crystalline phases, and represent excellent materials for basic studies of this subject.<sup>4</sup> The chirality of cholesteric liquid crystalline polymers have been searched in chiral nematic celluloses by Gray and coworkers and many other researchers<sup>5–13</sup>.

Ogura and coworkers have reported chitosan mesophase at concentrated solutions (>40 wt.%) in 10% aqueous acetic acid. Acetoxypolychitosan and hydroxypolychitosan were also used in this study.<sup>14</sup> Sakurai and coworkers studied liquid-crystalline structure in chitosan films and fibers prepared from liquid crystalline solutions.<sup>15–17</sup> Terbojevich and coworkers determined the persistence length of chitosan to be  $22 \pm 2$  nm in 0.1 mol/L CH<sub>3</sub>COOH + 0.2 mol/L NaCl in liquid crystalline phase.<sup>18</sup> Rout and coworkers found cholesteric solutions in PhCh and 3,6-di-*O*-acetyl-*N*-phtha-

\* Corresponding author. Tel.: +86-592-2182446; fax: +86-592-2188054.

E-mail address: [ymdong@xmu.edu.cn](mailto:ymdong@xmu.edu.cn) (Y. Dong).

loylchitosan dissolved in organic solvents.<sup>19–21</sup> Dong and coworkers demonstrated the lyotropic liquid crystallinity of more chitosan derivatives and studied the structure factors such as molecular weight, degree of deacetylation (D.D.), degree of substitution and the size of substituent, which influenced the critical concentration forming the liquid crystal phase.<sup>22–29</sup> Hu and coworkers reported the thermotropic phase transition in the chitosan/dichloroacetic acid system.<sup>30</sup> But so far, few authors investigated the handedness of chitosan and its derivatives.

In this study, we now report on the presence of two levels of chiral structure and the change of both helices for PhCh solutions in organic solvents by means of circular dichroism spectropolarimetry (CD).

## 2. Experimental

### 2.1. Preparation of (1→4)-2-deoxy-2-phthalimido-β-D-glucopyranan (*N*-phthaloylchitosan, PhCh)

PhCh was prepared as described.<sup>19</sup> Commercial reagent grade chitosan with a viscosity-average molecule weight ( $M_v$ ) of  $7.4 \times 10^5$  and a D.D. of 84% (measured with acid–base titration), as supplied by Xiamen Second Pharmaceutical Factory (China), was treated with 50% aq NaOH solution under  $N_2$  at 80 °C for 8 h three times to produce acetyl-free chitosan with a  $M_v$  of  $2.6 \times 10^5$ . The  $M_v$  was determined in 0.1 mol/L  $CH_3COONa$  + 0.2 mol/L  $CH_3COOH$  at 30 °C, according to the Mark–Houwink equation.  $K = 1.424 \times 10^{-3}$ ,  $\alpha = 0.96$  for D.D. = 84%; and  $K = 16.8 \times 10^{-3}$ ,  $\alpha = 0.81$  for D.D. = 100%.<sup>31</sup> Phthaloyl anhydride (18.0 g) and DMF (320 mL) were added into a flask, followed by 4.0 g acetyl-free chitosan (molecular ratio  $n_{\text{anhy}}:n_{\text{NH}_2} = 5:1$ ). The mixtures were stirred at 120 °C under nitrogen atmosphere for 7 h until a clear homogenous solution was achieved. Distilled deionized water (400 mL) was then poured into the above solution to precipitate the polymer. The precipitate was collected through filtering, and then washed with EtOH and water, respectively for several times. The wet outcome was dried under diminished pressure below 70 °C to give about 7.1 g of product.

### 2.2. Characterization of acetyl-free chitosan and PhCh

Acetyl-free chitosan was confirmed from the negligible intensity of the  $\nu(C=O)$  absorption band at about  $1650\text{ cm}^{-1}$  (amide band) in the Fourier-transform infra-red spectroscopy (FTIR) (Nicolet Avator 360, KBr) spectrum of chitin (Fig. 1).

The structure of PhCh was characterized by means of FTIR and  $^1\text{H}$  nuclear magnetic resonance ( $^1\text{H}$  NMR). The spectra are shown in Figs. 1 and 2. The data were as

follows. FTIR (Nicolet Avator 360, KBr):  $\nu(C=O)$   $1715(s)$  and  $1772\text{ cm}^{-1}(m)$ ,  $\nu(\text{benzene ring C-H})$   $722(m)$ .  $^1\text{H}$  NMR (Varian Unity NMR 500 MHz,  $CD_3SOCD_3$ , ppm):  $\delta$  3.0–4.5 (s, H-2–H-6, 6 H), 4.5–5.5 (m, H-1, 1 H), 7.2–8.0 (s, benzene ring, 4 H). Absence of substitution on oxygen was confirmed from the negligible intensity of absorption of  $\nu(C=O)$  in ester group at about  $1730\text{ cm}^{-1}$  in the FTIR spectrum of PhCh. The degree of substitution for PhCh was 1.0 from the results of  $^1\text{H}$  NMR.

### 2.3. CD determination

A JASCO CD spectropolarimeter, model J-810 was employed with band width 1 nm, data pitch 0.1 nm, scanning speed 200 nm/min, time constant 1 s and temperature 25 °C. The PhCh solution in  $Me_2SO$ , DMF or *N,N*-dimethylacetamide (DMAc) were prepared in small vials, which were tightly sealed. The solutions were aged for 3 days at room temperature and made homogenous in an oven at 100 °C for 10 min before use. A small portion of the solutions was placed between two quartz sheets, one of which being fitted with a round concavity in the center to keep the thickness of solutions as similar as possible ( $\sim 0.5\text{ mm}$ ).

### 2.4. Solubility of PhCh

PhCh can dissolve in many organic solvents, but can not dissolve in acidic solvents in contrast with chitosan. The solubility of PhCh was listed in Table 1. Three kinds of good solvents, i.e.,  $Me_2SO$ , DMF and DMAc, were used in this study.

## 3. Results and discussion

### 3.1. Lyotropic liquid crystalline behavior of PhCh solutions

All three kinds of PhCh solutions demonstrated liquid crystal phase in suitably high concentration. Fig. 3(a) shows a planar texture for a 55 wt.% PhCh/ $Me_2SO$  solution. The cholesteric phase usually demonstrates a planar texture, when the axes of spirals are almost vertical to the sample plane. Fig. 3(b) shows a banded texture of 55 wt.% PhCh/ $Me_2SO$  solution after shearing. It proves that this concentrated solution was a mesophase. In general, the system formed a lyotropic liquid crystal with a molecular weight distribution at two critical concentrations:  $C_1$  and  $C_2$ . Below  $C_1$ , the solution was isotropic, between  $C_1$  and  $C_2$ , the solution was a mixture of isotropic and anisotropic phases, and above  $C_2$ , the solution was fully anisotropic. In this study,  $C_1$  and  $C_2$  were measured both by polarized optical microscopy (POM, Olympus BH2) and small

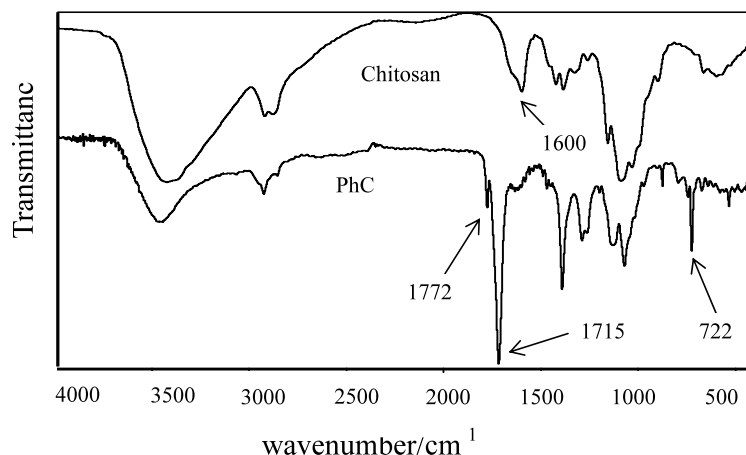
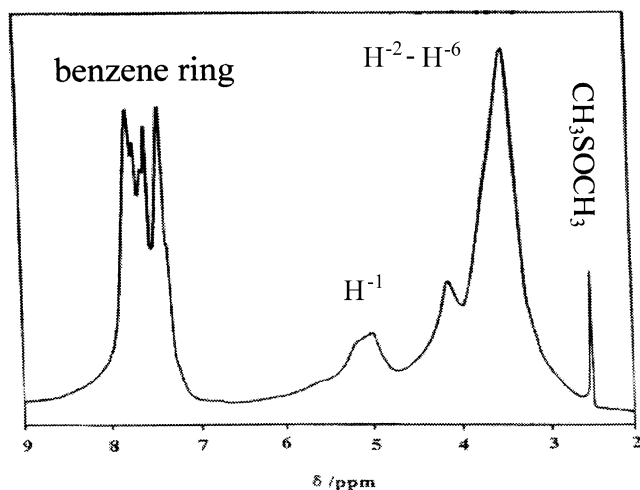


Fig. 1. FTIR spectra of acetyl-free chitosan and PhCh.

Fig. 2.  $^1\text{H}$  NMR spectrum of PhCh.

angle laser light scattering (SALS, instrument LS-1). Fig. 4(a) shows the SALS pattern with four leaves for the biphasic region because of the formation of anisotropic droplets in the background of isotropic phase. On the other hand, Fig. 4(b) shows the SALS pattern of symmetrical circle for the fully anisotropic phase. The results were listed in Table 2. For three kinds of solvents, both  $C_1$  and  $C_2$  were close, respectively. But the biphasic gap ( $C_2-C_1$ ) for the liquid crystal-to-isotropic phase transformation varied from 6 to 12 wt.% for the three systems.

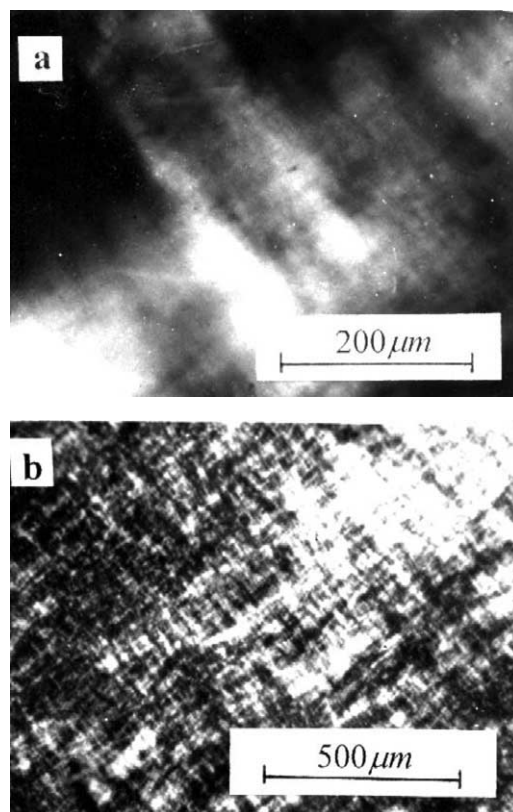
Fig. 3. Photomicrographs of the textures of 55 wt.% PhCh/ $\text{Me}_2\text{SO}$  solutions under crossed polars: (a) planar texture; (b) banded texture (after shearing).

Table 1  
The solubility of PhCh and chitosan

Solvent	Formic acid	$\text{Me}_2\text{SO}$	DMF	DMAc	Pyridine	Dioxane	$\text{Me}_2\text{CO}$	THF	$\text{CHCl}_3$	EtOAc
Chitosan	++	—	—	—	—	—	—	—	—	—
PhCh	—	++	++	++	+	+-	—	+	++	+

++, easily soluble; +, soluble; +-, swellable; —, unsolvable.

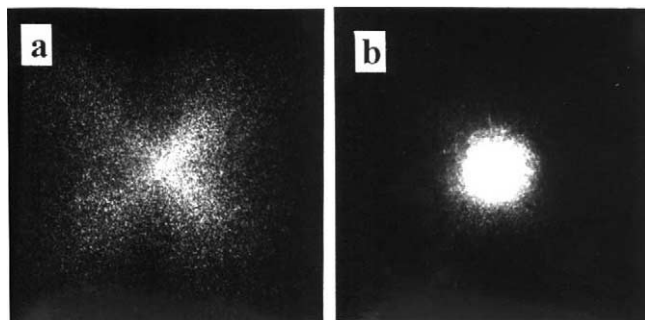


Fig. 4. SALS patterns of PhCh/Me<sub>2</sub>SO solutions at concentration of 45 (a) and 55 wt.% (b). The sample-to-film distance was 10 cm.

Table 2  
The critical concentrations of PhCh solutions

Solvent	C <sub>1</sub> (wt.%)	C <sub>2</sub> (wt.%)
Me <sub>2</sub> SO	43	55
DMAc	45	52
DMF	48	54

### 3.2. Two levels of chiral structure and their change of sign in PhCh/Me<sub>2</sub>SO solutions

From Fig. 5, it can be observed that there are two kinds of CD peaks, i.e., sharp peaks with absorption maximum at about 330 nm and broad peaks with absorption maximum at around 380 nm, which tail into almost the

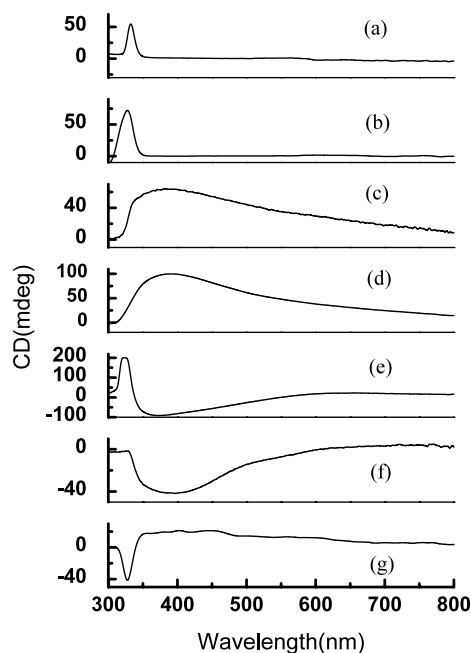


Fig. 5. CD spectra of PhCh/Me<sub>2</sub>SO solutions with varying concentrations: (a) 25; (b) 40; (c) 45; (d) 50; (e) 55; (f) 60; (g) 65 wt.%.

whole visible light region. The latter peaks only happened at the concentration higher than the critical concentration to form mesophase (43 wt.% for this system as measured by POM). So, the observation of broad absorption peaks may correspond to the appearance of a liquid crystalline phase. They arose from the selective reflection of cholesteric helix pitch. On the other hand, the former peaks occurred from very low concentration (1 wt.%) to high concentration, although they disappeared at some concentration. The sign of these peaks can change, implying the sense of twist reversed because only the helicoidal conformation of chains can vary its sense of twist except cholesteric helices, and the optical active carbon atoms in the fixed configuration of PhCh are not able to inverse the sign of CD. The observation of sharp absorption peaks does not arise due to the co-existence of chromophoric groups (phthaloyl side groups) and chiral carbon atom in chain, but may have its origin from the co-existence of chromophoric groups and helicoidal conformation of molecular chains.

From Fig. 5, the variation of sign for both kinds of peaks can also be noted. The negative or positive peak generally corresponded to the right- or left-handedness of the helicoidal molecular- and super-molecular structure, respectively. Consequently, the change in sign refers to the change in handedness.<sup>4,13</sup> The left-handed twist of both two kinds of helix, i.e., cholesteric helix of liquid crystalline phase and helicoidal conformation of molecular chain, all reverted to the right-handed one. It is interesting to notice that a left-handed helicoidal conformation and a right-handed cholesteric helix appeared at the same time at a concentration of 55 wt.% (see Fig. 5e). The helicoidal conformations almost disappeared in Fig. 5(c and d) and completely disappeared in Fig. 5(f). It can be explained by the formation of extended chain without twist. Inversion of the handedness has been reported in cellulose forming lyotropic cholesteric mesophases.<sup>4–13</sup> According to the theoretical consideration of Kimura and coworkers,<sup>32</sup> the observation of the twist sense of the supermolecular structures leads directly to the handedness of the chain conformation. So, it is not difficult to understand that the inversion of handedness for both cholesteric helix and helicoidal conformation of PhCh happened almost at the same time. Strictly speaking, the change of the former is slightly earlier than that of the latter with the increase of concentration. It is said that the handedness transfer occurred between these two levels of helicoidal structure. At very high concentration (65 wt.% showing in Fig. 5g), heavy light scattering occurred, so that large noise appeared with concomitant difficulty of measurement in the visible light region. The reason that the helicoidal conformations at the molecular level depended on the concentration is unclear. It is reported that in all conformational studies for cellulose, only

left-handed helices are established, since the conformation energy is lower for the left-handed structure.<sup>4</sup> So the right-handed helices of PhCh chains could only occur in the solution of higher concentration, in which the interaction of the chains was larger to stabilize higher energy conformation.

### 3.3. Change of handedness in PhCh/DMF solutions

Fig. 6 shows the influence of concentration on helicoidal structures in PhCh/DMF solutions. The effects were similar to PhCh/Me<sub>2</sub>SO system. The difference was that the broad peaks begin to appear at 50 wt.% (see Fig. 6c), because the critical concentration of lyotropic liquid crystal was 48 wt.% for this system. Moreover, the change of sign for the sharp peak appeared in 55 wt.%. No significant change of sign for the broad peaks was observed until 55 wt.%. These results implied that the handedness of helicoidal conformation of chain reversed from left- to right-handed as the concentration increased, but the handedness of cholesteric helix of liquid crystalline phase did not. The latter may happen at higher concentration, but unfortunately we cannot observe it because of the difficulty of experiment. Heavy light scattering occurred at very high concentration (60

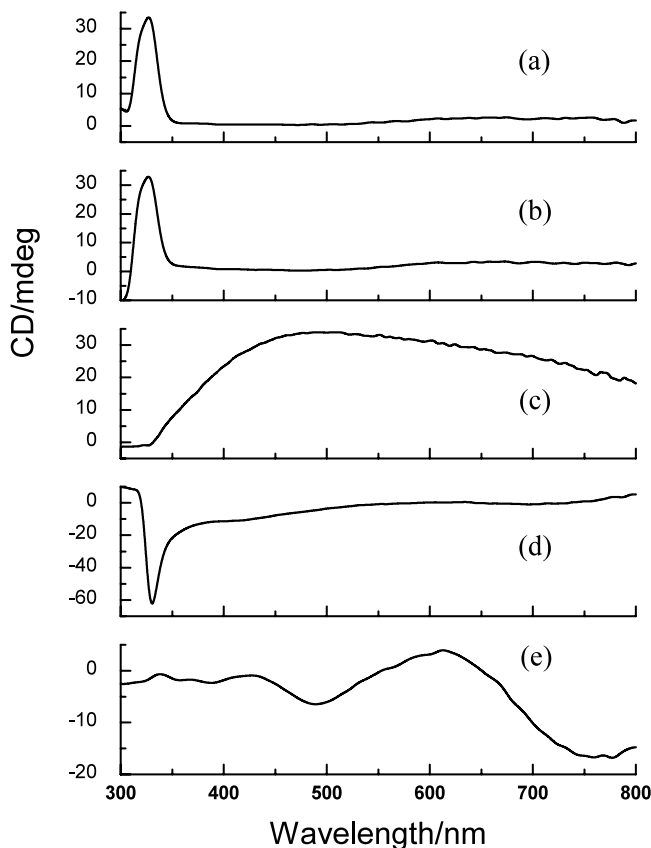


Fig. 6. CD spectra of PhCh/DMF solutions at varying concentrations: (a) 35; (b) 45; (c) 50; (d) 55; (e) 60 wt.%.

wt.%), with high noise. The spectrum (Fig. 6e) became no meaningful.

### 3.4. Change of handedness in PhCh/DMAc solutions

Fig. 7 shows the influence of concentration on helicoidal structures in PhCh/DMAc solutions. The effects were similar to PhCh/DMF system, but there were two differences. Firstly, the broad peaks began to appear at 45 wt.% (Fig. 7c), because the critical concentration of lyotropic liquid crystal is 45 wt.% for this system. Secondly, the change of sign for the sharp peak appeared at 62 wt.% (Fig. 7g), and also the maximum of the sharp peak moved slightly to 320 nm. No significant change of sign for the broad peaks was observed until 60 wt.%. The solutions with very high concentration (more than 65 wt.%) were also difficult to determine due to the above mentioned reason (Fig. 7h).

It is of interest to note that there was a dramatical variation of CD spectra, when the concentration was close to the critical concentration  $C_1$ . When the concentration was 43 wt.%, there was no broad peak at all (Fig. 8a). But the broad peak with the maximum at

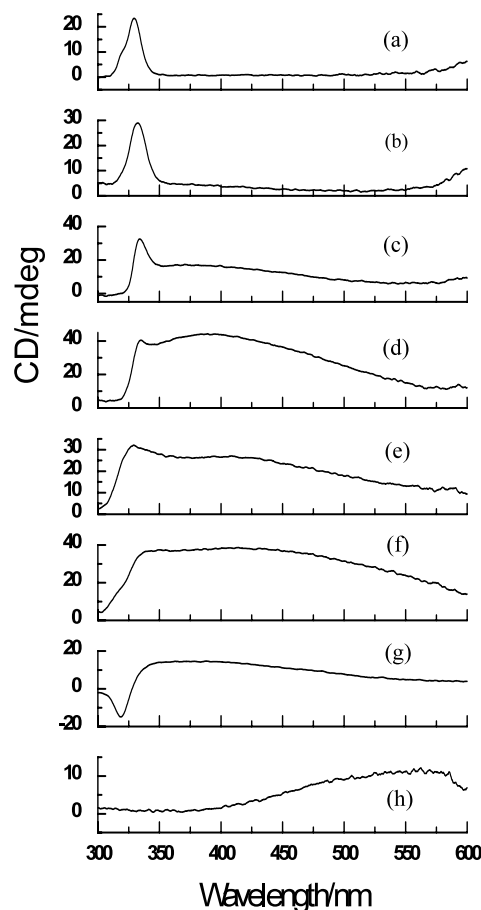


Fig. 7. CD spectra of PhCh/DMAc solutions at varying concentrations: (a) 5; (b) 40; (c) 45; (d) 50; (e) 55; (f) 60; (g) 62; (h) 65 wt.%.



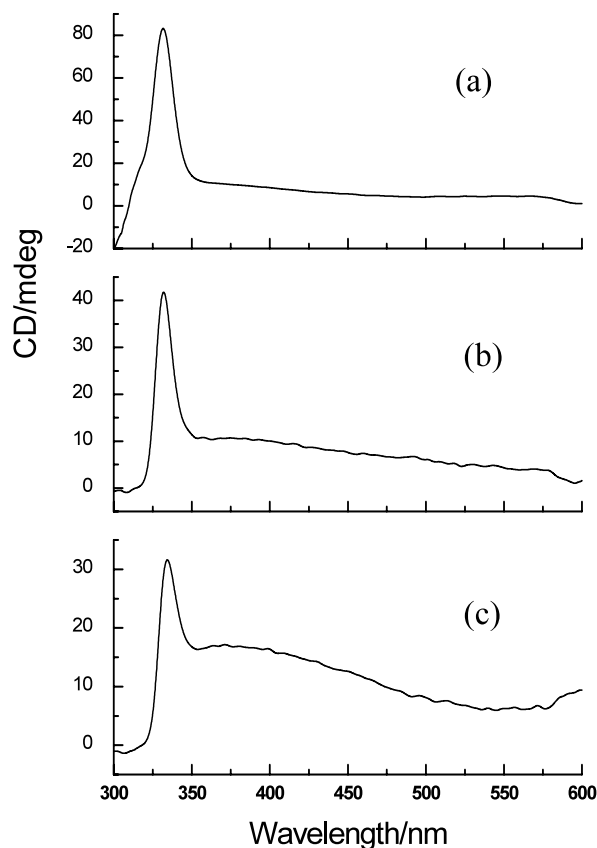


Fig. 8. CD spectra of PhCh/DMAc solutions at concentrations near the critical concentration (45 wt.%): (a) 43; (b) 44; (c) 45 wt.%.

about 380 nm just started to appear at the concentration of 44 wt.% (Fig. 8b). Subsequently the broad peak became very evident in the slightly higher concentration of 45 wt.% (Fig. 8c). So the critical concentration must be 44 wt.% from this results of CD. But the critical concentration measured by POM was 45 wt.% as mentioned previously. No birefringence was observed in the solution of 44 wt.% with POM. Therefore, we can conclude that CD is more sensitive to measure critical concentration of lyotropic cholesteric phase than POM with regard to the system PhCh/DMAc.

It seemed that the change of sign in CD spectra did not certainly relate to  $C_2$ , although for PhCh/Me<sub>2</sub>SO system the sign of Cotton effect of the broad peak happened to change in 55 wt.%, which matched  $C_2$ .

### 3.5. Further discussion

From CD determination, the variation of two levels of chiral structure, i.e., twisted layer structure at the supermolecule level and the helicoidal conformation at the molecule level, was observed in mesophase of PhCh solutions. A schematic illustration of these two levels of chiral structure is shown in Fig. 9. The change and

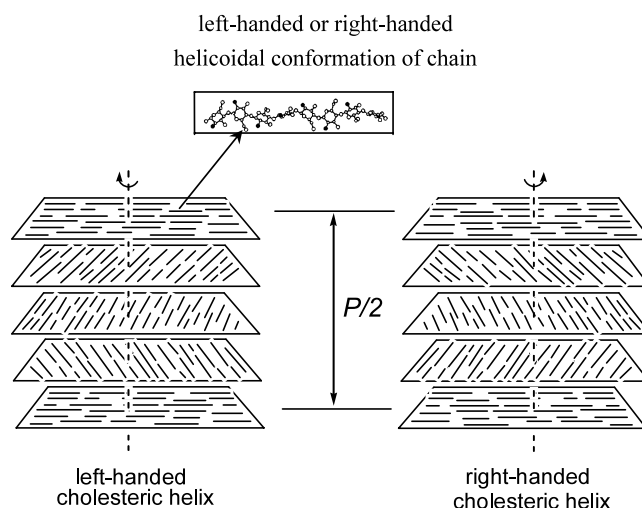


Fig. 9. Schematic illustration of the relationship between cholesteric helix and helicoidal conformation of chain.

transfer of handedness of PhCh solutions happened in these two levels of chiral structure.

The CD peaks induced by cholesteric helix were usually broader as compared with the CD observation of cellulose. No obvious color induced by the selective reflection can be seen. Moreover, the cholesteric pitch values are normally sensitive to the concentration for cellulose. But from Figs. 5–7, no evident shift of absorption maximum can be noticed. So it seemed that the cholesteric phase formed in PhCh/Me<sub>2</sub>SO, PhCh/DMF and PhCh/DMAc solutions consisted of only short-range ordered domains which do not show uniform cholesteric macroscopic helices as Rout and coworkers explained previously.<sup>19</sup> Also, the cholesteric pitch values have a wide distribution in these poorly ordered domains.

### Acknowledgements

This investigation was supported by the National Nature Science Foundation of China (No. 29974023).

### References

1. Roberts, G. A. F. *Chitin Chemistry*; Macmillan Press Ltd: London, 1992; p 1.
2. Kurita, K.; Ichikawa, H.; Ishizeki, S.; Fujisaki, H.; Iwakawa, Y. *Makromol. Chem. Phys.* **1982**, *183*, 1161–1169.
3. Nishimura, S. I.; Kohgo, O.; Kurita, K.; Kuzuhara, H. *Macromolecules* **1991**, *24*, 4745–4748.
4. Zugenmaier, P. In *Handbook of Liquid Crystals*; Demus, D.; Goodby, J.; Gray, G. W.; Spiess, H. V.; Vill, V., Eds. *High Molecular Weight Liquid Crystal*; Vol. 3; Wiley-VCH: New York, 1998; pp 453–482.

5. Guo, J. X.; Gray, D.G. In: Gilbert R.D. (Ed.), *Cellulosic Polymers*, Hanser Munich, 1994, p. 25.
6. Vogt, U.; Zugenmaier, P. *Ber. Bunsenges. Phys. Chem.* **1985**, *89*, 1217–1224.
7. Pawlowski, W. P.; Gilbert, R. D. *J. Polym. Sci. Polym. Phys. Ed.* **1987**, *25*, 2293–2301.
8. Ritcey, A. M.; Gray, D. G. *Macromolecules* **1988**, *21*, 1251–1255.
9. Ritcey, A. M.; Holme, K. R.; Gray, D. G. *Macromolecules* **1988**, *21*, 2914–2917.
10. Guo, J. X.; Gray, D. G. *Macromolecules* **1989**, *22*, 2082–2085.
11. Guo, J. X.; Gray, D. G. *Macromolecules* **1989**, *22*, 2086–2090.
12. Harkness, B. R.; Gray, D. G. *Can. J. Chem.* **1990**, *68*, 1135–1139.
13. Suto, S. Inoue. *M. Polymer.* **1999**, *40*, 2455–2457.
14. Ogura, K.; Kanamoto, T.; Sannan, T.; Tanaka, K.; Iwakura Y, Proc. 2nd Int Conf Chitin/Chitosan, Tottori, Japan, 1982, pp. 39–44.
15. Sakurai, K.; Shibano, T.; Kimura, K.; Takahashi, T. *Sen-i. Gakkaishi.* **1985**, *41*, 361–368.
16. Sakurai, K.; Takahashi, T. *Sen-i. Gakkaishi.* **1988**, *93*, 147–151.
17. Sakurai, K.; Miyata, M.; Takahashi, T. *Sen-i. Gakkaishi.* **1990**, *46*, 79–81.
18. Terbojevich, M.; Cosani, A.; Conio, G.; Marsano, E.; Bianchi, E. *Carbohydr. Res.* **1991**, *209*, 251–260.
19. Rout, D. K.; Pulapura, S. K.; Gross, R. A. *Macromolecules* **1993**, *26*, 5999–6006.
20. Rout, D. K.; Pulapura, S. K.; Gross, R. A. *Macromolecules* **1993**, *26*, 6007–6010.
21. Rout, D. K.; Barman, S. P.; Pulapura, S. K.; Gross, R. A. *Macromolecules* **1994**, *27*, 2945–2950.
22. Dong, Y.; Li, Z. *Chin. J. Polym. Sci.* **1999**, *17*, 65–70.
23. Dong, Y.; Wang, J.; Quan, Y. *Chin. J. Polym. Sci.* **2000**, *18*, 15–17.
24. Dong, Y.; Quan, Y.; Wu, Y.; Wang, M. *J. Appl. Polym. Sci.* **2000**, *76*, 2057–2061.
25. Dong, Y.; Qiu, W.; Ruan, Y.; Wu, Y.; Wang, M.; Xu, C. *Polym. J.* **2001**, *33*, 387–389.
26. Dong, Y.; Wu, Y.; Wang, J.; Wang, M. *Eur. Polym. J.* **2001**, *37*, 1713–1720.
27. Dong, Y.; Xu, C.; Wang, J.; Wu, Y.; Ruan, Y.; Wang, M. *Polym. Bull.* **2001**, *45*, 495–500.
28. Dong, Y.; Xu, C.; Wang, J.; Wu, Y.; Wang, M.; Ruan, Y. *J. Appl. Polym. Sci.* **2002**, *83*, 1204–1205.
29. Wu, Y.; Dong, Y.; Ling, C.; Huang, J.; Jun, L. *Macromol. Biosci.* **2002**, *2*, 131–134.
30. Hu, Z.; Li, R.; Wu, D.; Sun, Y.; Liu, H.; Wu, L. *Chem. J. Chin. Univ.* **1999**, *1*, 153–155.
31. Wang, W.; Bo, S.; Qin, W. *Zhongguo. Kexue. (Ser. B)* **1990**, *11*, 1131–1226.
32. Kimura, H.; Hosina, M.; Nakano, H. *J. Phys. (Jpn)* **1982**, *51*, 1584–1590.